Modeling of the Media Supply of Gas Burners of an Industrial Furnace

authored by **C. Froehlich, S. Strommer, A. Steinboeck, M. Niederer, and A. Kugi**

and published in *IEEE Transactions on Industry Applications*.

Cite this article as:

C. Froehlich, S. Strommer, A. Steinboeck, M. Niederer, and A. Kugi, "Modeling of the media supply of gas burners of an industrial furnace", *IEEE Transactions on Industry Applications*, vol. 52, no. 3, pp. 2664–2672, May 2016. DOI: 10.1109/TIA.2016.2521738

BibTex entry:

```
@Article{acinpaper,
  Title = {Modeling of the Media Supply of Gas Burners of an Industrial Furnace},
  Author = {C. Froehlich and S. Strommer and A. Steinboeck and M. Niederer and A. Kugi},
  Journal = {IEEE Transactions on Industry Applications},
  Year = {2016},

  Month = {May},
  Number = {3},
  Pages = {2664--2672},
  Volume = {52},

  Doi = {10.1109/TIA.2016.2521738},
  Url = {http://ieeexplore.ieee.org/xpl/articleDetails.jsp?arnumber=7393541}
}
```

Contact:

Automation and Control Institute (ACIN)
Vienna University of Technology
Gusshausstrasse 27-29/E376
1040 Vienna, Austria

Internet: www.acin.tuwien.ac.at
E-mail: office@acin.tuwien.ac.at
Phone: +43 1 58801 37601
Fax: +43 1 58801 37699

Modeling of the Media-Supply of Gas Burners of an Industrial Furnace

Christoph Froehlich, Stephan Strommer, Andreas Steinboeck, Martin Niederer and Andreas Kugi
Automation and Control Institute (ACIN)
TU Wien
Gusshausstrasse 27-29, 1040 Vienna, Austria
{froehlich, strommer, steinboeck, niederer, kugi}@acin.tuwien.ac.at

***Abstract*—Gas-fired industrial furnaces are used to heat products to a predefined temperature level. As the temperature of the load as well as the composition of the flue gas are crucial for many applications in industry, the controllers of burners have to ensure a given heat input and air-fuel ratio. As a basis for such controllers, an accurate mathematical model of the media supply of an industrial furnace, including valves, pressure reducing valves, and long hot-air pipelines, will be derived from first principles and verified by means of measured data of a real plant[1].**

***Index Terms*—Mathematical model, System identification, Fluid flow, Furnaces, Least squares approximations, Pipelines, Temperature, Thermal analysis, Finite element analysis, Valves**

I. Introduction

In the steel industry, gas-fired furnaces are often used to heat steel products for annealing or for further processing like rolling. The furnace being considered is part of a production process of flat steel products. Here, the mass flows of the fuel gas and the combustion air serve as control inputs for a superimposed temperature controller. The furnace has two operating modes that differ in terms of the fuel-gas composition: fuel-lean and fuel-rich mixtures. The latter is used to prevent scale formation on the product surface as a consequence of oxygen-free flue gas. A controller has to prevent unwanted switching between these two modes, i. e., an accurate control of the air-fuel ratio is critical for safety reasons and for the product quality. In this work, a mathematical model of the media supply network will be derived. It can be used as a basis for control design. Hence, the model should capture the essential dynamic behavior of the system and it should be computationally inexpensive.

A. Media supply of gas burners

In Figure 1, the media supply of the considered furnace is outlined. Fuel gas and combustion air are separately fed to the nozzle mix burner. Natural gas is used as fuel. It is supplied by a transfer station and expanded by a pressure reducing valve (PRV in Figure 1) to a defined operating pressure p_f. The fuel gas flow control valve regulates the mass flow $\dot{m}_f$ to the furnace, which then heats up the steel products. Additionally, a bypass line maintains a minimum mass flow to prevent an extinction of the flame. If required, a shut-off valve can be used to completely stop the supply of natural gas.

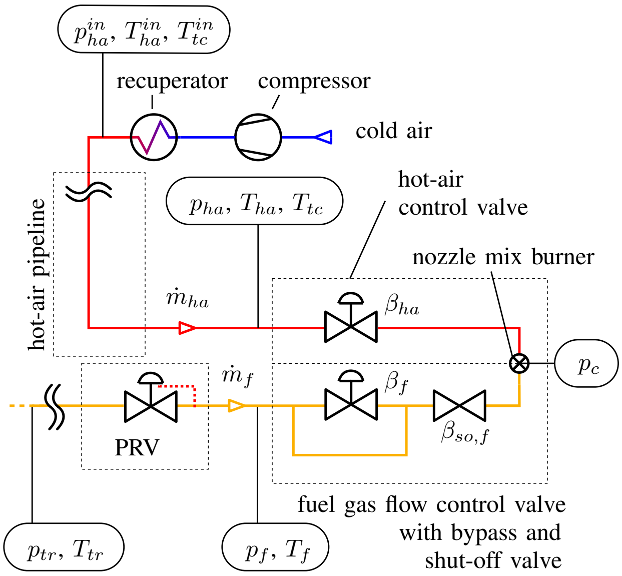

Fig. 1: Media supply of a nozzle mix burner.

As a second medium for the combustion, ambient air is sucked into the media supply by a compressor. To reduce the consumption of fuel gas, the combustion air is preheated by means of a recuperator. It recovers thermal energy from the flue gas leaving the furnace. The recuperator does not need to be considered in the present work because the temperature T_{ha}^{in} and the pressure p_{ha}^{in} of the hot air leaving the recuperator are measured. The heated air then passes through an insulated hot-air pipeline which is several dozens of meters long. Along this pipeline, the air exchanges thermal energy with the environment leading to a change of its temperature. A hot-air flow control valve defines the mass flow $\dot{m}_{ha}$ of the air.

[1] This research was partially supported by the Austrian Research Promotion Agency (FFG), Grant No.: 834305. The third author gratefully acknowledges financial support provided by the Austrian Academy of Sciences in the form of an APART-fellowship (Austrian Programme for Advanced Research and Technology) at the Automation and Control Institute of TU Wien.
This work has been presented at the IEEE IAS Annual Meeting 2015 in Dallas, TX [1]

Post-print version of the article: C. Froehlich, S. Strommer, A. Steinboeck, M. Niederer, and A. Kugi, "Modeling of the media supply of gas burners of an industrial furnace", *IEEE Transactions on Industry Applications*, vol. 52, no. 3, pp. 2664–2672, May 2016. DOI: 10.1109/TIA.2016.2521738
The content of this post-print version is identical to the published paper but without the publisher's final layout or copy editing.

B. Existing models

To describe the states of transient pipe flows, several approaches are available in the literature. A short overview will be given here:

The most accurate but computationally expensive method is *computational fluid dynamics* (CFD). Due to the high computational effort, it is not useful for model-based control design [2], [3]. Neglecting thermodynamical effects, a MATLAB/SIMULINK library was used to model long gas pipelines [4]. The pipes in the considered media supply network are of shorter length and thermodynamical effects should not be neglected. Another possibility is to employ the analogy between electrical networks and pipe networks [5]. This method uses a simplification of resistances in the fluid system and assumes isothermal gas flow.

Glueck et al. [6] presented a mathematical model of a pneumatic system. Neglecting pipe friction, this model describes the flow and the thermodynamic behavior of the compressible fluids. Pipes with constant surface temperatures are assumed. Gölles et al. [7] proposed a model of a biomass furnace with incompressible fluids neglecting thermodynamic interaction between the fluids and the environment.

Further, a model of the PRV has to be developed to describe the mass flow in the fuel gas branch. Parker and White [8] studied the steady-state characteristics of a pneumatic pressure regulator. Tsai and Cassidy [9] proposed a dynamical model of PRVs where an idealized behavior for the pressure drop was assumed.

During an earlier study of the presented furnace, a less detailed simulation model of the media supply was developed [10]. In this study, the hot-air pipeline, the PRVs in the natural gas pipeline, and the compressibility of the fluid have not been considered.

Additionally, a transient thermodynamical model to describe the temperature loss along the hot-air pipeline has to be derived. The governing partial differential equations (PDEs) could be solved by *finite difference methods* (FDMs) [11]. To solve these PDEs with less effort, weighted residual methods, e. g., the Galerkin method, can be used. Steinboeck et al. [12] derived a fast simulation model for one-dimensional heat conduction. Yu et al. [13] also presented a simulation model for underground oil pipelines by means of the Galerkin method.

C. Motivation for this work

The superordinate controller for the temperature of the steel product assumes an ideal behavior of the media supply. Therefore, an accurate control of the mass flows is crucial to allow for high product quality and to ensure a safe operation of the furnace. Thus, a model-based control for the media supply may be useful. Additionally, the possibility to operate the furnace at its limits, i. e. with highest heat input at dynamic load variations, seems promising. For this, an accurate mathematical model with low computational effort is required. None of the models proposed in the literature meet these requirements. Moreover, the proposed model can also be beneficial for other purposes:

- training of operators
- tool for design decisions
- recuperating more thermal energy without overstressing the heat exchanger

D. Contents

The present work is structured as follows: In Section II, a mathematical model of the media supply of a nozzle mix burner is derived by first principles. In Section III, the system is validated and compared to measured data from a real plant at *voestalpine Stahl GmbH*, Linz, Austria and Section IV contains some conclusions.

II. MATHEMATICAL MODELING

A mathematical model of the pipe network shown in Figure 1 is derived. It consists of several submodels which are defined first. The most important process variables are the mass flows, the temperatures, and the pressures of the streaming fluids, i. e., hot air and fuel gas. Both fluids are modeled as compressible and ideal gases. With the exception of the hot-air pipeline, all pipe flows are assumed to be isothermal.

A. Orifice flow

The description of the mass flow $\dot{m}$ through a valve is based on a sharp-edged orifice [14], [15]. Assuming frictionless adiabatic flow without the supply of specific work, the mass flow is given by

$$\dot{m} = C p_1 \rho_0 \sqrt{T_0/T_1}\, \Psi(\Pi) \ . \tag{1}$$

Here, $\Pi = p_2/p_1$ is the pressure ratio, p_1 the upstream pressure, p_2 the downstream pressure, T_1 the upstream temperature, C the so-called discharge coefficient, ρ_0 the mass density of the fluid at a reference temperature T_0, and $\Psi(\Pi) = \sqrt{1-\left(\frac{\Pi-b}{1-b}\right)^2}$ a normalized approximation of the discharge function for $b < \Pi < 1$. Below the so-called critical pressure ratio

$$b = \Pi_{krit} := \left(\frac{2}{\kappa+1}\right)^{\frac{\kappa}{\kappa-1}} \tag{2}$$

with the adiabatic index κ of the fluid, a further decrease of Π does not result in an increase of $\dot{m}$. This case is called choked-flow, i. e., $\Psi(\Pi) = 1$ for $0 < \Pi < b$. The real critical pressure ratio b is smaller than the theoretical value according to (2) and consequently, a constant value $b = \Pi_{krit}/2$ is used. Caused by the low upstream pressures p_1 in the pipe network, $\Pi = p_2/p_1 > b$ always holds and the case with choked flow is neglected. Analytical formulations of a constant discharge coefficient C are available [14], [15]. However, C is not constant over the whole operating range and a relation of the form $C = C(\Pi, \beta)$ can be used, where β is the valve position. Therefore, measured values from the real plant $(p_1^i, p_2^i, \dot{m}^i, T_1^i)$ are used to calculate the discharge coefficients at the sampling instances i, i. e., $C_{meas}^i = \dot{m}^i \Big/ \left(p_1^i \rho_0 \sqrt{T_0/T_1^i}\sqrt{1-\left(\frac{\Pi^i-b}{1-b}\right)^2}\right)$. Then, a polynomial in Π and β is fitted by applying the least-squares method to approximate $C(\Pi, \beta)$. Figure 2 shows measured values as crosses, while the surface represents the identified polynomial $C(\Pi, \beta)$.

Post-print version of the article: C. Froehlich, S. Strommer, A. Steinboeck, M. Niederer, and A. Kugi, “Modeling of the media supply of gas burners of an industrial furnace”, *IEEE Transactions on Industry Applications*, vol. 52, no. 3, pp. 2664–2672, May 2016. DOI: 10.1109/TIA.2016.2521738
The content of this post-print version is identical to the published paper but without the publisher’s final layout or copy editing.

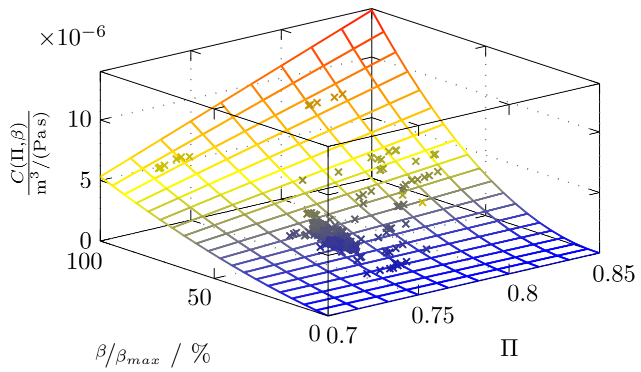

Fig. 2: Identified discharge characteristics of a valve.

B. Valve dynamics

The valves are controlled by subordinate position controllers, which use auxiliary pneumatic systems. Figure 3 shows the desired valve position β_{sp} and the actual time evolution β of a typical valve of the considered plant. Clearly, the dynamic response is characterized by a dead time. A

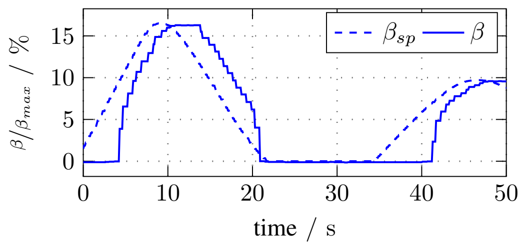

Fig. 3: Poppet valve with actuator dead time.

simplified semi-empirical dynamical model is given in the form of a first-order low pass with a constant dead time T_{DT}, i. e.,

$$\dot{\beta} = \frac{1}{\tau}\left(K\beta_{sp}\left(t - T_{DT}\right) - \beta\right) \ . \tag{3}$$

Here, potential feedback forces of the streaming fluid on the valve are neglected. The time constant τ, the dead time T_{DT}, and the gain K can be identified by means of measured data of the respective valve. For this purpose, the optimization problem

$$\min_{\tau, T_{DT}, K} \sum_i \left(\beta^i - \beta^i_{sim}\left(\tau, T_{DT}, K\right)\right)^2 \tag{4}$$

is solved. Here, β^i_{sim} is the output of the simulated system (3) and β^i is the corresponding measured value at the sampling instance i.

C. Pressure reducing valves

To provide the system with fuel gas at a fixed pressure level, mechanical pressure reducing valves (PRVs) are used. Figure 4 shows the configuration of a typical PRV. The measurement diaphragm, which is pretensioned by a setpoint spring, compares the ambient pressure p_∞ with the downstream pressure

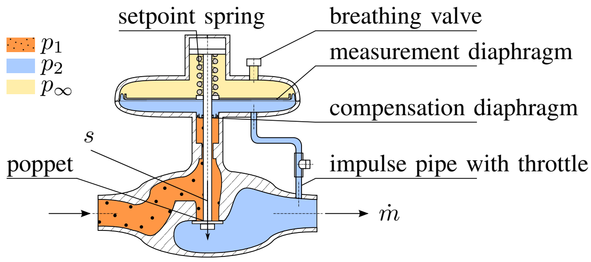

Fig. 4: Pneumatic PRV including a return spring.

p_2, and holds the poppet of the valve at the position s. The compensation diaphragm eliminates the static pressure forces on the poppet. Thus, the poppet position is independent of the upstream pressure p_1. Due to the design of the poppet, steady-state flow forces are negligible [16] and the downstream pressure is a function of the form $p_2 = f\left(\dot{m}, s\left(p_2\right)\right)$. Measured data show that the valve reacts immediately and without overshooting (sufficient damping) upon changes of the mass flow $\dot{m}$. This justifies the use of a quasi steady-state model of the PRV. Because the poppet positions cannot be measured without extra sensor equipment, it is omitted in the model proposed here. Similar to (1), the steady-state model of a PRV reads as

$$\dot{m} = C_{prv}\left(p_1, p_2\right) p_1 \rho_0 \sqrt{{T_0}/{T_1}}\, \Psi_{prv}\left({p_2}/{p_1}\right) \tag{5}$$

with the upstream pressure p_1, the upstream temperature T_1, the downstream pressure p_2, and the mass density ρ_0 at a reference temperature T_0. The discharge coefficient $C_{prv}\left(p_1, p_2\right)$ of a PRV is a function of p_1 and p_2 and can be identified in a similar way as described in Section II-A. Considering a polytropic temperature change, the downstream temperature T_2 follows as

$$T_2 = T_1 \left({p_2}/{p_1}\right)^{\frac{n-1}{n}} \tag{6}$$

with the polytropic exponent $n \in (1, \kappa)$. Note that n is chosen such that (6) describes measured temperature changes in an accurate way.

D. Pressure drop in a long pipeline

Based on the Reynolds number

$$Re := \frac{vL}{\nu} \tag{7}$$

with a characteristic length L, an average fluid velocity v, and the kinematic viscosity ν of the fluid, it can be argued that the pipe flows in the considered media supply system are always turbulent. For this flow regime and compressible fluids, the pressure drop Δp reads as

$$\Delta p = p_1 - p_2 = p_1\left(1 - \sqrt{1 - \zeta\frac{L}{D}\frac{\rho_1}{2}v_1^2\frac{\left(T_1 + T_2\right)}{p_1 T_1}}\right) \tag{8}$$

with the upstream pressure p_1, the upstream temperature T_1, the downstream pressure p_2, the downstream temperature T_2, a characteristic length L, the diameter D of the channel, the dimensionless coefficient ζ called Moody friction factor, the mass density ρ_1, and the mean velocity v_1 at the inlet [3],

Post-print version of the article: C. Froehlich, S. Strommer, A. Steinboeck, M. Niederer, and A. Kugi, "Modeling of the media supply of gas burners of an industrial furnace", *IEEE Transactions on Industry Applications*, vol. 52, no. 3, pp. 2664–2672, May 2016. DOI: 10.1109/TIA.2016.2521738
The content of this post-print version is identical to the published paper but without the publisher's final layout or copy editing.

[17]. As Petukhov [18] suggested, an approximate relation for turbulent flows is

$$\zeta = (0.79 \ln(Re) - 1.64)^{-2} \ . \tag{9}$$

E. Transient thermal model for a long pipeline

Figure 5 shows a cross-section of an insulated pipeline with length L, inner radius r_i and outer radius r_o. The pipe is surrounded by ambient air with the temperature T_∞ and a fluid with the mass flow $\dot{m}$ and the input temperature T_{ha}^{in} streams through the pipe. The fluid temperature $T_g(z,t)$ changes due to heat exchange with the pipe (heat flux $\dot{q}_i(z,t)$). The outlet temperature $T_g(z = L, t) = x_1(t)$ is of interest. The wall temperature $T_w(r,z,t)$ is $T_{w,i}(z,t)$ at the inner surface and $T_{w,o}(z,t)$ at the outer surface. There the heat flux $\dot{q}_o(z,t)$ is present.

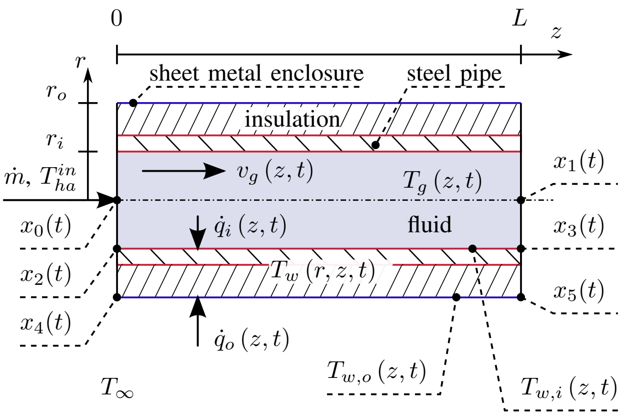

Fig. 5: Cross section of the hot-air pipeline.

1) Problem formulation: Heat conduction mainly occurs in radial direction because the temperature gradient in radial direction is much higher than in longitudinal direction. This is why the heat equation in cylindrical coordinates is used for the domain $(r,z) \in \Omega_W = (r_i, r_o) \times (0, L]$ [19]. It reads as

$$\mathscr{D}(T_w) = \rho_w(r) c_w(r) \frac{\partial T_w}{\partial t} - \frac{1}{r}\frac{\partial}{\partial r}\left(r k_w(r) \frac{\partial T_w}{\partial r}\right) = 0 \ . \tag{10a}$$

The considered pipe wall consists of three layers: an inner steel pipe, a mineral wool insulation, and a sheet metal enclosure, see Figure 5. Each layer is characterized by its mass density ρ_w, specific heat capacity c_w, and thermal conductivity k_w. Let the initial temperature distribution be

$$T_w(r,z,t=0) = T_{w0}(r,z) \ . \tag{10b}$$

The heat transfer on the wall surfaces is convective. Hence, the boundary conditions read as

$$\mathscr{B}_i(T_w) = -k_w \left.\frac{\partial T_w}{\partial r}\right|_{r=r_i} - \dot{q}_i = 0 \tag{10c}$$

$$\mathscr{B}_o(T_w) = k_w \left.\frac{\partial T_w}{\partial r}\right|_{r=r_o} - \dot{q}_o = 0 \tag{10d}$$

with

$$\dot{q}_i(z,t) = \alpha_i (T_g(z,t) - T_{w,i}(z,t)) \tag{11a}$$

$$\dot{q}_o(z,t) = \alpha_o (T_\infty - T_{w,o}(z,t)) \ . \tag{11b}$$

The orientations of the heat fluxes $\dot{q}_i$ and $\dot{q}_o$ are shown in Figure 5. The calculation of the heat transfer coefficients α_i and α_o will be discussed later.

By using the energy balance and applying Reynold's transport theorem [3], [19], the differential equation governing the gas temperature $T_g(z,t)$ follows as

$$\mathscr{D}_g(T_g, T_{w,i}) = \frac{\partial T_g}{\partial t} + v_g \frac{\partial T_g}{\partial z} + \frac{2 r_i \pi}{A \rho_g c_{p,g}} \dot{q}_i = 0 \tag{12a}$$

subject to the boundary condition

$$T_g(z=0,t) = T_{ha}^{in}(t) \tag{12b}$$

and initial condition

$$T_g(z, t=0) = T_{g0}(z) \ , \tag{12c}$$

respectively. Here, ρ_g is the mass density calculated from the ideal gas law, $c_{p,g}$ is the specific heat capacity of the fluid, $A = r_i^2 \pi$ is the cross-sectional area, and v_g is the mean fluid velocity.

2) Convection: The heat transfer coefficients α_i and α_o are computed from the Nusselt number

$$Nu := \frac{\alpha L_0}{k} \ , \tag{13}$$

where L_0 is a characteristic length and k is the thermal conductivity of the fluid. Moreover,

$$Pr := {}^{\nu}/_{a} \tag{14}$$

is the Prandtl number, where a is the thermal diffusivity of the fluid. For forced convection in smooth tubes with $L/D \geq 10$, the empirical relation

$$Nu = \frac{\zeta/8 \, (Re - 1000) \, Pr}{1 + 12.7\sqrt{\zeta/8}\left(Pr^{\frac{2}{3}} - 1\right)} \tag{15}$$

with ζ from (9) is suggested [20]. With (7), (13) – (15), and $v = v_g = {}^{\dot{m}}/_{(\rho_g r_i^2 \pi)}$, α_i follows as a function of $\dot{m}$.

Free convection occurs on the outer surface. For this configuration and Rayleigh numbers in the range of

$$Ra := Gr Pr \lesssim 10^{12} \ , \tag{16}$$

the approximate relation

$$Nu = \left(0.6 + \frac{0.387 Ra^{1/6}}{1 + \left(0.559/Pr\right)^{9/16}\right)^{8/27}}\right)^2 \tag{17}$$

with the Grashof number

$$Gr := \frac{g \beta L_0^3 \left|T_{w,o} - T_\infty\right|}{\nu^2} \tag{18}$$

is used [20]. Here, g is the gravitational acceleration, $T_{w,o}$ the surface temperature, and $\beta = \frac{1}{T_\infty}$ is the thermal expansion coefficient of an ideal gas. Eq. (13), (14), and (16) – (18) are used to calculate α_o.

Post-print version of the article: C. Froehlich, S. Strommer, A. Steinboeck, M. Niederer, and A. Kugi, "Modeling of the media supply of gas burners of an industrial furnace", *IEEE Transactions on Industry Applications*, vol. 52, no. 3, pp. 2664–2672, May 2016. DOI: 10.1109/TIA.2016.2521738
The content of this post-print version is identical to the published paper but without the publisher's final layout or copy editing.

If the burners are shut off, the fluid is not in motion, i. e., $\dot{m} = 0$ or $v_g = 0$ and free convection occurs also on the inner pipe surface. In this case, the temperature evolution of the pipe wall is of interest to obtain the initial condition when valves are opened again. Here, the gas temperature itself is of smaller significance, because the evolution of the pipe wall temperature is mainly influenced by the pipe wall itself due to its high heat capacity. Due to simplicity reasons, (17) is also used to calculate α_i for $\dot{m} = 0$.

3) Solution by means of Galerkin method: Because an analytical solution of the PDEs (10a) and (12a) is difficult to find, an approximate solution scheme is used. By applying the Galerkin weighted residual method [21], the temperature distribution is approximated by a finite number of discrete system states $x_l, l = 0, \dots, 5$, shown in Figure 5. The approximation involves two steps: First, the dependence of $T_w(r, z, t)$ on r is approximated by $T_{w,i}(z, t)$ and $T_{w,o}(z, t)$. Then, the dependence of $T_{w,i}(z, t)$, $T_{w,o}(z, t)$, and $T_g(z, t)$ on the longitudinal coordinate z is approximated using the states x_l. As an appropriate trial function in radial direction, the steady-state solution of (10a) is employed. For a wall consisting of N layers, the steady-state temperature distribution within layer $m = 1, \dots, N$, i. e., $r \in [r_{i,m}, r_{i,m+1}]$, takes the form

$$\tilde{T}_w(r, z) = \tilde{T}_{w,i}(z)\,\phi_i(r) + \tilde{T}_{w,o}(z)\underbrace{\frac{\sum_{l=1}^{m-1}\frac{\ln\left(r_{i,l+1}/r_{i,l}\right)}{k_{w,l}} + \frac{\ln\left(r/r_{i,m}\right)}{k_{w,m}}}{\sum_{l=1}^{N}\frac{\ln\left(r_{i,l+1}/r_{i,l}\right)}{k_{w,l}}}}_{\phi_o(r)} \tag{19}$$

with $\phi_i(r) = 1 - \phi_o(r)$. Here, $r_{i,m}$ is the inner radius of the layer m, $r_{i,1} = r_i$, $r_{i,N+1} = r_o$, and $k_{w,m}$ is the uniform thermal conductivity of the layer m. The functions ϕ_i and ϕ_o are used as trial functions for the approximate solution in the layer m

$$\hat{T}_w(r, z, t) = T_{w,i}(z, t)\,\phi_i(r) + T_{w,o}(z, t)\,\phi_o(r) \tag{20}$$

for $r \in [r_{i,m}, r_{i,m+1}]$. $T_{w,i}(z, t)$ and $T_{w,o}(z, t)$ follow from the weighted residuals equations

$$\int_{r_i}^{r_o} \phi_i(r)\,\mathscr{D}\left(\hat{T}_w\right)\mathrm{d}r + \underbrace{\phi_i(r_i)}_{=1}\mathscr{B}_i\left(\hat{T}_w\right) + \underbrace{\phi_i(r_o)}_{=0}\mathscr{B}_o\left(\hat{T}_w\right) = 0 \tag{21a}$$

$$\int_{r_i}^{r_o} \phi_o(r)\,\mathscr{D}\left(\hat{T}_w\right)\mathrm{d}r + \underbrace{\phi_o(r_i)}_{=0}\mathscr{B}_i\left(\hat{T}_w\right) + \underbrace{\phi_o(r_o)}_{=1}\mathscr{B}_o\left(\hat{T}_w\right) = 0 \tag{21b}$$

with $\mathscr{D}$, $\mathscr{B}_i$, and $\mathscr{B}_o$ from (10). This yields

$$\frac{\partial}{\partial t}\begin{bmatrix} T_{w,i}(z,t) \\ T_{w,o}(z,t) \end{bmatrix} = \overbrace{\begin{bmatrix} C_{w1} & C_{w2} \\ C_{w2} & C_{w3} \end{bmatrix}^{-1}}^{=:\mathbf{\Gamma}} \underbrace{\begin{bmatrix} \dot{q}_i(z,t) - T_{w,i}(z,t)\,A_{w,i} - T_{w,o}(z,t)\,A_{w,o} \\ \dot{q}_o(z,t) - T_{w,i}(z,t)\,B_{w,i} - T_{w,o}(z,t)\,B_{w,o} \end{bmatrix}}_{=:\mathbf{f}(T_{w,i},T_{w,o})=[f_1(T_{w,i},T_{w,o}),f_2(T_{w,i},T_{w,o})]^{\mathrm{T}}} . \tag{22}$$

If the integrals are evaluated piecewise with ϕ_i and ϕ_o within the respective layer m, the calculation of the entries of $\mathbf{C}_w$ and $\mathbf{f}$, i. e. $C_{wl}, l \in \{1, 2, 3\}$ and $A_{wl}, B_{wl}, l \in \{i, o\}$, is fairly straightforward, e. g.,

$$\begin{aligned} C_{w3} &= \int_{r_i}^{r_o} c_w(r)\rho_w(r)\left(\phi_o(r)\right)^2 \mathrm{d}r \\ &= \sum_{m=1}^{N} \int_{r_{i,m}}^{r_{i,m+1}} c_{w,m}\,\rho_{w,m}\left(\phi_o(r)\right)^2 \mathrm{d}r . \end{aligned} \tag{23}$$

Here, $c_{w,m}$ and $\rho_{w,m}$ are uniform within the respective layer m.

To find trial functions for the direction z, the steady-state solution of (12a), i. e.,

$$\frac{\partial \tilde{T}_g}{\partial z} = -\frac{2r_i\pi}{\dot{m}c_{p,g}}\tilde{\dot{q}}_i , \tag{24}$$

is solved first. The steady-state heat flux $\tilde{\dot{q}}_i(z)$ in (24) can be calculated from the steady-state solution of (22), i. e., from $\mathbf{f} = \mathbf{0}$. This yields

$$\tilde{\dot{q}}_i(z) = \tilde{T}_{w,i}(z)\,A_{w,i} + \tilde{T}_{w,o}(z)\,A_{w,o} \tag{25a}$$

$$\tilde{\dot{q}}_o(z) = \tilde{T}_{w,i}(z)\,B_{w,i} + \tilde{T}_{w,o}(z)\,B_{w,o} . \tag{25b}$$

Using (11b) and (25b) $T_{w,o}$ and $\dot{q}_o$ can be eliminated. With the abbreviations

$$c_1 = A_{w,i} - \frac{A_{w,o}B_{w,i}}{B_{w,o} + \alpha_o}, c_2 = \frac{\alpha_o A_{w,o}}{B_{w,o} + \alpha_o} ,$$

and (25a) follows

$$\tilde{T}_{w,i}(z) = \frac{1}{c_1}\tilde{\dot{q}}_i(z) + \frac{c_2}{c_1}T_\infty . \tag{26}$$

This result can be inserted into (11a), which gives

$$\tilde{\dot{q}}_i(z) = \frac{\alpha_i}{1 + \frac{\alpha_i}{c_1}}\left(\tilde{T}_g(z) + \frac{c_2}{c_1}T_\infty\right) . \tag{27}$$

Insertion into (24) yields the linear ODE

$$\frac{\partial \tilde{T}_g}{\partial z} = -\underbrace{\frac{2r_i\pi}{\dot{m}c_{p,g}}\frac{\alpha_i}{1 + \frac{\alpha_i}{c_1}}}_{:=\chi}\left(\tilde{T}_g + \frac{c_2}{c_1}T_\infty\right) . \tag{28}$$

Its exact solution can be easily computed. However, only the shape of this solution is of interest. Clearly, this shape is defined by $\exp(-\chi z)$. The solution of (28) and the equations (11), (25), and (26) show that the steady-state solutions $\tilde{T}_{w,i}$, $\tilde{T}_{w,o}$, $\tilde{\dot{q}}_i$, and $\tilde{\dot{q}}_o$ also contain the expression $\exp(-\chi z)$. Based on this observation, the approximate solutions

$$\hat{T}_g(z, t) = x_0(t)\sigma_0(z) + x_1(t)\sigma_1(z) \tag{29a}$$

$$\hat{T}_{w,i}(z, t) = x_2(t)\sigma_0(z) + x_3(t)\sigma_1(z) \tag{29b}$$

$$\hat{T}_{w,o}(z, t) = x_4(t)\sigma_0(z) + x_5(t)\sigma_1(z) \tag{29c}$$

are chosen with the trial functions

$$\sigma_1(z) = \frac{1 - \mathrm{e}^{-\chi z}}{1 - \mathrm{e}^{-\chi L}} \tag{30a}$$

$$\sigma_0(z) = 1 - \sigma_1 = \frac{\mathrm{e}^{-\chi z} - \mathrm{e}^{-\chi L}}{1 - \mathrm{e}^{-\chi L}} . \tag{30b}$$

Post-print version of the article: C. Froehlich, S. Strommer, A. Steinboeck, M. Niederer, and A. Kugi, "Modeling of the media supply of gas burners of an industrial furnace", *IEEE Transactions on Industry Applications*, vol. 52, no. 3, pp. 2664–2672, May 2016. DOI: 10.1109/TIA.2016.2521738
The content of this post-print version is identical to the published paper but without the publisher's final layout or copy editing.

The parameter χ (cf. (28)) is calculated once for a typical operating point and then held constant. The Galerkin coefficients $x_l(t), l = 1, \ldots, 5$ are chosen so that based on $\mathscr{D}_g(T_g, T_{w,i})$ from (12a) and

$$\mathscr{D}_i\left(\hat{T}_{w,i}, \hat{T}_{w,o}\right) = \frac{\partial \hat{T}_{w,i}}{\partial t} - \Gamma_{1,1} f_1\left(\hat{T}_{w,i}, \hat{T}_{w,o}\right) - \Gamma_{1,2} f_2\left(\hat{T}_{w,i}, \hat{T}_{w,o}\right) = 0 \tag{31a}$$

$$\mathscr{D}_o\left(\hat{T}_{w,i}, \hat{T}_{w,o}\right) = \frac{\partial \hat{T}_{w,o}}{\partial t} - \Gamma_{2,1} f_1\left(\hat{T}_{w,i}, \hat{T}_{w,o}\right) - \Gamma_{2,2} f_2\left(\hat{T}_{w,i}, \hat{T}_{w,o}\right) = 0 \tag{31b}$$

from (22), where $\Gamma_{i,j}, i, j = 1, 2$ refer to the entries of $\mathbf{\Gamma}$, the five weighted residuals

$$\int_0^L \sigma_1(z)\, \mathscr{D}_g\left(\hat{T}_g, \hat{T}_{w,i}\right) \mathrm{d}z = 0 \tag{32a}$$

$$\int_0^L \sigma_\psi(z)\, \mathscr{D}_\gamma\left(\hat{T}_{w,i}, \hat{T}_{w,o}\right) \mathrm{d}z = 0 \tag{32b}$$

with $\psi \in \{0, 1\}, \gamma \in \{i, o\}$ become zero. Solving (32) yields

$$\dot{x}_1 = C_g^{-1}\left(-A_{g1}x_1 + A_{g2}x_2 + A_{g3}x_3 - A_{g,in}x_0\right) \tag{33a}$$

$$\begin{bmatrix}\dot{x}_2\\ \dot{x}_3\end{bmatrix} = \mathbf{C}_i^{-1}\left(\mathbf{A}_{i,in}\begin{bmatrix}x_2\\ x_3\end{bmatrix} + \mathbf{B}_{i,out}\begin{bmatrix}x_4\\ x_5\end{bmatrix} + \mathbf{B}_{i,g}\begin{bmatrix}x_0\\ x_1\end{bmatrix} + \mathbf{b}_{i,\infty}T_\infty\right) \tag{33b}$$

$$\begin{bmatrix}\dot{x}_4\\ \dot{x}_5\end{bmatrix} = \mathbf{C}_o^{-1}\left(\mathbf{A}_{o,in}\begin{bmatrix}x_2\\ x_3\end{bmatrix} + \mathbf{B}_{o,out}\begin{bmatrix}x_4\\ x_5\end{bmatrix} + \mathbf{B}_{o,g}\begin{bmatrix}x_0\\ x_1\end{bmatrix} + \mathbf{b}_{o,\infty}T_\infty\right) \tag{33c}$$

with $x_0 = T_{ha}^{in}$ as system input and the initial values $x_l(t = 0) = x_{l0}, l = 1, \ldots, 5$. A list of the constants used in (33) can be found in [22]. Based on (33), the temperature evolution of the gas and the pipe wall can be easily calculated.

If $\dot{m} = 0$ holds, the temperature evolution is determined to obtain feasible initial conditions when the valves open again. In this case, (12b) cannot be used. However, the same trial functions (30) are employed. The additional unknown state variable (gas temperature) $T_g(0, t) = x_0(t)$ and the additional weighted residual

$$\int_0^L \sigma_0(z)\, \mathscr{D}_g\left(\hat{T}_g, \hat{T}_{w,i}\right) \mathrm{d}z = 0 \tag{34}$$

have to be considered. Hence, (33a) is replaced by

$$\begin{bmatrix}\dot{x}_0\\ \dot{x}_1\end{bmatrix} = \tilde{\mathbf{C}}_g^{-1}\tilde{\mathbf{A}}_g\left(\begin{bmatrix}x_0\\ x_1\end{bmatrix} - \begin{bmatrix}x_2\\ x_3\end{bmatrix}\right) . \tag{35}$$

For calculating α_i and α_o according to Section II-E2 and ρ_g by means of the ideal gas law, average temperatures of the wall surfaces and the gas are determined in the form

$$\bar{T}_\phi(t) = \frac{1}{L}\int_0^L \hat{T}_\phi(z, t)\,\mathrm{d}z\,, \qquad \phi \in \{{}_{w,o}, {}_{w,i}\, , {}_g\} . \tag{36}$$

F. Thermocouple

Thermocouples covered by a ceramic shield are used to measure the gas temperature as shown in Figure 6. Due to the radiative interaction with the pipe wall and the heat capacity of the thermocouple itself, the measured temperature T_{tc} may deviate from the true gas temperature T_g [23], [24]. To compensate for this error, a dynamic model of T_{tc} is derived. A simple heat balance yields

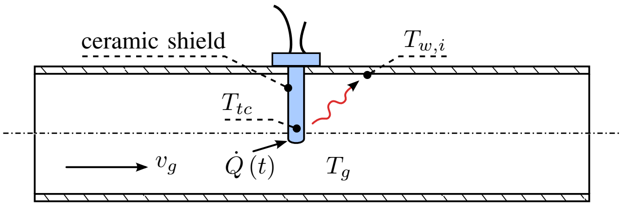

Fig. 6: Thermocouple inside a pipe.

$$\frac{\mathrm{d}T_{tc}}{\mathrm{d}t} = \frac{1}{m_{tc}c_{tc}}\dot{Q}(t) \tag{37}$$

with the mass m_{tc} and the specific heat capacity c_{tc} of the thermocouple. The heat flow

$$\dot{Q}(t) = A_{tc}\alpha_i\left(T_g - T_{tc}\right) + A_{tc}\sigma\varepsilon_{tc}\left(T_{w,i}^4 - T_{tc}^4\right) \tag{38}$$

via the surface of the thermocouple consists of a convective and a radiative part. Here, T_g is the local gas temperature, $T_{w,i}$ is the local inner pipe wall temperature, A_{tc} is the surface area of the thermocouple inside the pipe, σ is the Stefan-Boltzmann constant, ε_{tc} is the radiative emissivity, and the heat transfer coefficient α_i is assumed to be the same as on the inner pipe surface.

G. Full model

Now, the mathematical model of the considered pipe network according to Figure 1 can be presented. For this, recall that the indices $_{ha}$ and $_f$ are used for the hot-air and the fuel gas subsystem, respectively.

The dynamic behavior of the system switches depending on the fact if hot air is streaming through the hot-air pipeline ($\dot{m}_{ha} > 0$) or not ($\dot{m}_{ha} = 0$). If $\dot{m}_{ha} > 0$, the upstream gas temperature $x_0(t) = T_{ha}^{in}(t)$ is calculated according to Section II-F based on a thermocouple measurement T_{tc}^{in} at $z = 0$. Rearranging (37) and (38) yields

$$T_{ha}^{in} = \dot{T}_{tc}^{in}\frac{m_{tc}c_{tc}}{A_{tc}\alpha_i} + \frac{\sigma\varepsilon_{tc}}{\alpha_i}\left(\left(T_{tc}^{in}\right)^4 - x_2^4\right) + T_{tc}^{in}\,, \tag{39}$$

with the simulated inner pipe wall temperature x_2. The time derivative $\dot{T}_{tc}^{in}$ in (39) can be numerically calculated, e.g., by means of a Savitzky-Golay filter [25]. The equation (see (33a))

$$\dot{T}_{ha} = C_g^{-1}\left(-A_{g1}T_{ha} + A_{g2}x_2 + A_{g3}x_3 - A_{g,in}T_{ha}^{in}\right) \tag{40}$$

defines the ODE for the output temperature $x_1 = T_{ha}$ of hot air. If the pipeline is shut off ($\dot{m}_{ha} = 0$), the temperature change of the air in the pipeline can be described by (cf. (35))

$$\begin{bmatrix}\dot{x}_0\\ \dot{T}_{ha}\end{bmatrix} = \mathbf{C}_g^{-1}\mathbf{A}_g\left(\begin{bmatrix}x_0\\ T_{ha}\end{bmatrix} - \begin{bmatrix}x_2\\ x_3\end{bmatrix}\right) . \tag{41}$$

Post-print version of the article: C. Froehlich, S. Strommer, A. Steinboeck, M. Niederer, and A. Kugi, "Modeling of the media supply of gas burners of an industrial furnace", *IEEE Transactions on Industry Applications*, vol. 52, no. 3, pp. 2664–2672, May 2016. DOI: 10.1109/TIA.2016.2521738

The equations (33b) and (33c) hold true independent of $\dot{m}_{ha}$. Using (8), the pressure at the end of the hot-air pipeline follows in the form

$$p_{ha} = p_{ha}^{in}\sqrt{1-\zeta\frac{L}{2r_i}\frac{\rho_{ha}}{2}v_g^2\frac{(T_{ha}^{in}+T_{ha})}{p_{ha}^{in}T_{ha}^{in}}} \tag{42a}$$

with $v_g = \dot{m}_{ha}/(\rho_{ha}r_i^2\pi)$ and $\rho_{ha} = \rho_{0,ha}p_{ha}^{in}T_0/(T_{ha}^{in}p_0)$ from the ideal gas law. The temperature T_{tc} of the thermocouple, which is located at the end of the pipeline (cf. Figure 1), is calculated from (37) and (38), i. e.,

$$\dot{T}_{tc} = \frac{A_{tc}\alpha_i}{m_{tc}c_{tc}}(T_{ha}-T_{tc}) + \frac{A_{tc}\sigma\varepsilon_{tc}}{m_{tc}c_{tc}}\left(x_3^4 - T_{tc}^4\right) \tag{42b}$$

with the pipe wall temperature x_3 and the hot-air temperature T_{ha} at the location of the thermocouple. The position β_{ha} of the poppet of the hot-air flow control valve and β_f of the fuel gas control valve are calculated from (3). Considering the shut-off valve by an additional discrete input $\beta_{so,f} \in \{0,1\}$ ($\beta_{so,f} = 1$ for closed valve), the mass flow of the fuel gas follows from (1) in the form

$$\dot{m}_f = (1-\beta_{so,f})\, C_f\left(\frac{p_c}{p_f},\beta_f\right) p_f\rho_{0,f}\sqrt{\frac{T_0}{T_f}}\Psi_f\left(\frac{p_c}{p_f}\right) . \tag{42c}$$

The effect of the bypass line is captured by the discharge coefficient $C_f\left(\frac{p_c}{p_f},\beta_f\right)$. The mass flow $\dot{m}_{ha}$ of the hot air is described in a similar fashion from (1). The pressure p_f and the gas temperature T_f after the PRV (cf. Figure 1) can be computed from

$$\dot{m}_f = C_{prv}(p_{tr},p_f)\, p_{tr}\rho_{0,f}\sqrt{\frac{T_0}{T_{tr}}}\Psi_{prv}\left(\frac{p_f}{p_{tr}}\right) \tag{42d}$$

$$T_f = T_{tr}\left(\frac{p_f}{p_{tr}}\right)^{\frac{n-1}{n}} \tag{42e}$$

(cf. (5) and (6)).

The full mathematical model can be written as a differential-algebraic-system of the form

$$\dot{\mathbf{x}} = \mathbf{\Phi}(\mathbf{x},\mathbf{z},\mathbf{u}) , \qquad \mathbf{x}(t=0) = \mathbf{x}_{t0} \tag{43a}$$

$$\mathbf{0} = \mathbf{\Gamma}(\mathbf{x},\mathbf{z},\mathbf{u}) , \tag{43b}$$

where $\mathbf{x}^{\mathrm{T}} = [x_0, T_{ha}, x_2, x_3, x_4, x_5, T_{tc}, \beta_{ha}, \beta_f]$ is the state, $\mathbf{z}^{\mathrm{T}} = [p_{ha}, \dot{m}_{ha}, \dot{m}_f, p_f, T_f]$ is the vector of algebraic variables, and $\mathbf{u}^{\mathrm{T}} = \left[T_{tc}^{in}, p_{ha}^{in}, p_{tr}, T_{tr}, p_c, \beta_{sp,ha}, \beta_{sp,f}\right]$ is the system input.

III. Experimental validation

The proposed model is validated by means of measured data from the real plant.

First, the submodel (42d) is validated. Figure 7 shows the measured pressure p_f^* and its simulated counterpart p_f of the PRV (presented as gauge pressures), where the fuel gas mass flow $\dot{m}_f$, the upstream pressure p_{tr} and the upstream temperature T_{tr} serve as system inputs. Apart from measurement noise, the model output p_f and the measured time evolution p_f^* agree well. Furthermore, it can be seen that the downstream pressure p_f^* is only marginally influenced by variations in the upstream pressure p_{tr} but changes in the mass flow $\dot{m}_f$ cannot be fully compensated by the PRV.

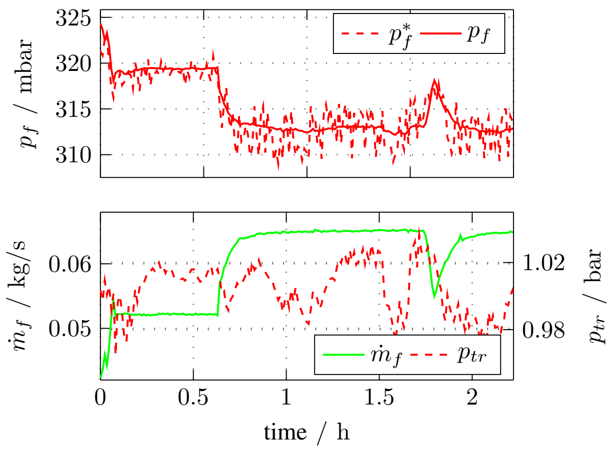

Fig. 7: Simulated and measured response of the PRV.

Next, the thermal model of the hot-air pipeline (40) – (42) is validated using measured gas temperatures. For comparison, the finite-difference method (FDM) is used to solve the PDEs as described in [22]. The Galerkin method simulates five times faster than the model derived by the FDM using fifty discretization points. The deviation between these two temperature models is below $T_w < 2\,\%$ (in K), which justifies the use of the faster Galerkin method. Figure 8 shows simulation results of the models (39), (40), and (42). The measured thermocouple reading T_{tc}^* is compared to the simulated signal T_{tc} for a scenario with given mass flow $\dot{m}_{ha}$ and input temperature T_{tc}^{in}. The absolute error $|\Delta T_{tc}| = |T_{tc} - T_{tc}^*|$ (in K) remains below $1\,\%$ K. This proves the capability of the

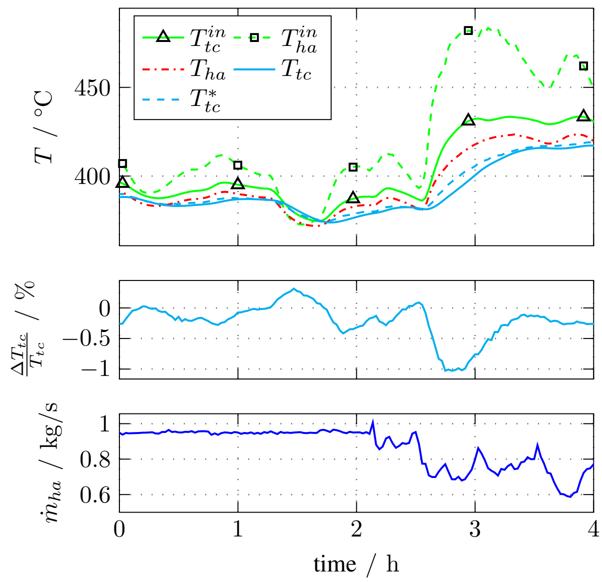

Fig. 8: Simulated and measured temperature of hot-air pipeline.

Post-print version of the article: C. Froehlich, S. Strommer, A. Steinboeck, M. Niederer, and A. Kugi, "Modeling of the media supply of gas burners of an industrial furnace", *IEEE Transactions on Industry Applications*, vol. 52, no. 3, pp. 2664–2672, May 2016. DOI: 10.1109/TIA.2016.2521738

model to capture cooling as well as heating of the streaming fluid.

Now the full model (43) is validated. Figure 9 shows the simulated mass flow $\dot{m}_{ha}$ of the hot-air branch compared to the measured mass flow $\dot{m}^*_{ha}$ together with the setpoint signal $\beta_{ha,sp}$ of the valve and the calculated upstream pressure p_{ha}. The simulated and measured signals $\dot{m}_{ha}$ and $\dot{m}^*_{ha}$ agree well

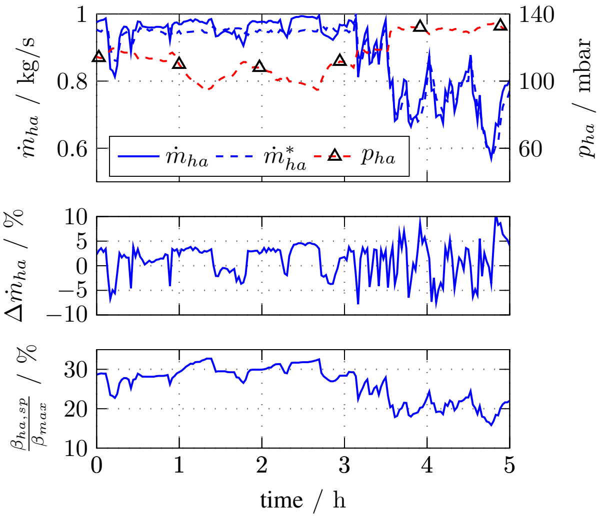

Fig. 9: Mass flows of the hot-air branch.

with a small error $\Delta\dot{m}_{ha} = \dot{m}_{ha} - \dot{m}^*_{ha}$.

Finally, the measured mass flow $\dot{m}^*_f$ and the simulated mass flow $\dot{m}_f$ of the fuel gas branch are shown in Figure 10. At the beginning (cf. left figure), the shut-off valve is closed, i. e., $\beta_{so,f} = 1$. The measured mass flow $\dot{m}^*_f$ shows that the

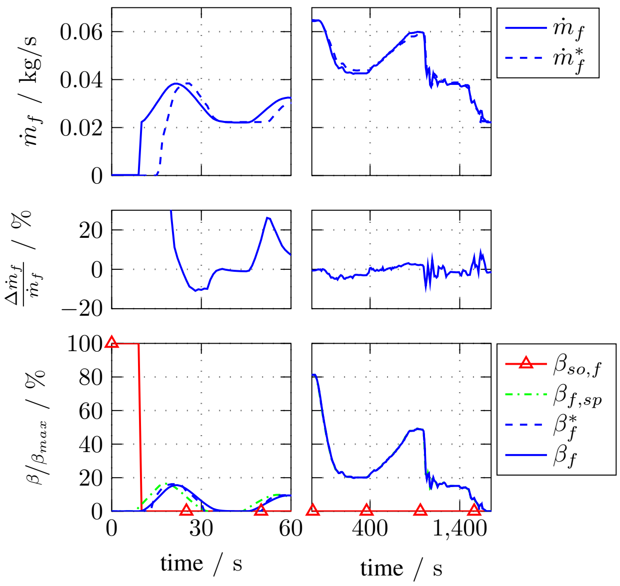

Fig. 10: Mass flows of the fuel gas branch.

shut-off valve also exhibits a small time delay, which is not captured by the model. Further, it can be seen that if the fuel gas flow control valve is opened from the fully-closed state its time delay T_{DT} is not constant. This partially explains the deviation $\Delta\dot{m}_f = \dot{m}_f - \dot{m}^*_f$. During normal operation, the system is very accurate (cf. right figure). Noteworthy errors $|\Delta\dot{m}_f| > 10\,\%$ only occur during rapid motion of the valve.

IV. Conclusion and Outlook

In this work, a mathematical model capable of describing the transient behavior of the media supply of a gas-fired industrial furnace as shown in Figure 1 was presented.

The transient temperature evolution of a gaseous fluid in a long, insulated pipeline can be accurately simulated with low computational effort. The full model was validated by measured data from the real plant. The most relevant process variables, the mass flows of fuel gas and combustion air, are accurately captured by the model. Therefore, the model serves as a good starting point for model-based analysis, control design and optimization.

Acknowledgment

The authors kindly express their gratitude to the industrial research partner voestalpine Stahl GmbH.

Christoph Froehlich (S'10) received the M.Sc. degree in automation technology from Vienna University of Technology, Austria, in 2015.

Since 2015 he is a research assistant with the Automation and Control Institute at Vienna University of Technology, Vienna, Austria. His research activities are within the fields of mathematical modeling, identification and control of nonlinear dynamical systems with applications in the steel industry as well as the polymer processing industry.

Stephan Strommer received the Dipl.-Ing. degree in electrical engineering form the Technische Universitaet Muenchen, Munich, Germany, in 2010.

Since 2011, he has been research assistant with the Automation and Control Institute at Vienna University of Technology, Vienna, Austria. His main research interests cover numerical methods in engineering, industrial furnaces, as well as modeling, optimization, and control of nonlinear dynamical systems.

Post-print version of the article: C. Froehlich, S. Strommer, A. Steinboeck, M. Niederer, and A. Kugi, "Modeling of the media supply of gas burners of an industrial furnace", *IEEE Transactions on Industry Applications*, vol. 52, no. 3, pp. 2664–2672, May 2016. DOI: 10.1109/TIA.2016.2521738
The content of this post-print version is identical to the published paper but without the publisher's final layout or copy editing.

Andreas Steinboeck received the M.Sc. degree in mechatronics from Loughborough University, Loughborough, U.K., in 2005, the Dipl.-Ing. degree in mechatronics from Johannes Kepler University, Linz, Austria, in 2007, and the Ph.D. (Dr. techn.) degree in electrical engineering from Vienna University of Technology, Austria, in 2011.

Since 2007, he has been a research assistant with the Automation and Control Institute at Vienna University of Technology, Vienna, Austria. His main research interests cover numerical methods in engineering, mechanical structures, stability analysis, mathematical modeling, identification, optimization and control of nonlinear dynamical systems, as well as applications in continuous production processes in the steel industry.

Martin Niederer received the Dipl.-Ing. degree in electrical engineering from the Vienna University of Technology, Austria, in March 2011.

Since March 2011 he works as a research assistant at the Automation and Control Institute (ACIN) at Vienna University of Technology. His main research interests include the physics-based modeling and the nonlinear control of annealing furnaces in the steel industry.

Andreas Kugi (M'94) received the Dipl.-Ing. degree in electrical engineering from Graz University of Technology, Austria, and the Ph.D. (Dr. techn.) degree in control engineering from Johannes Kepler University (JKU), Linz, Austria, in 1992 and 1995, respectively. He received his "Habilitation" degree in the field of automatic control and control theory from JKU in 2000.

From 1995 to 2000 he worked as an assistant professor and from 2000 to 2002 as an associate professor at JKU. In 2002, he was appointed full professor at Saarland University, Saarbrücken, Germany, where he held the Chair of System Theory and Automatic Control until May 2007. Since June 2007 he is a full professor for complex dynamical systems and head of the Automation and Control Institute (ACIN) at TU Wien, Austria. His research interests include the physics-based mathematical modeling, control and optimization of nonlinear dynamical systems with a strong focus on industrial applications.

Dr. Kugi is full member of the Austrian Academy of Sciences and Editor-in-Chief of the Control Engineering Practice.

References

[1] C. Froehlich, S. Strommer, A. Steinboeck, M. Niederer, and A. Kugi, "Modeling of the media-supply of gas burners of an industrial furnace," in *Proceedings of the IEEE Industry Applications Society Annual Meeting*, 2015, pp. 1–9.

[2] J. Wendt, Ed., *Computational Fluid Dynamics*, 3rd ed. Berlin, Heidelberg: Springer, 2009.

[3] Y. A. Çengel, R. H. Turner, and J. M. Cimbala, *Fundamentals of thermal-fluid sciences*, 4th ed. Boston: McGraw-Hill Education, 2012.

[4] M. Behbahani-Nejad and A. Bagheri, "A MATLAB Simulink library for transient flow simulation of gas networks," *World Academy of Science, Engineering and Technology*, vol. 2, no. 7, pp. 139–145, 2008.

[5] S. L. Ke and H. C. Ti, "Transient analysis of isothermal gas flow in pipeline network," *Chemical Engineering Journal*, vol. 76, no. 2, pp. 169–177, 2000.

[6] T. Glück, W. Kemmetmüller, P. Zanolin, and A. Kugi, "Dreistufiger Kolbenkompressor mit vorgeschaltetem Drehkolbenkompressor: Teil 1, Modellierung," *at – Automatisierungstechnik*, vol. 60, no. 12, pp. 766–775, 2012.

[7] M. Gölles, S. Reiter, T. Brunner, N. Dourdoumas, and I. Obernberger, "Model based control of a small-scale biomass boiler," *Control Engineering Practice*, vol. 22, pp. 94–102, 2014.

[8] G. Parker and D. White, "Modeling the steady-state characteristics of a single-stage pneumatic pressure regulator," *Fluidics Quarterly*, vol. 9, no. 2, pp. 23–46, 1977.

[9] D. H. Tsai and E. C. Cassidy, "Dynamic behavior of a simple pneumatic pressure reducer," *Journal of Fluids Engineering*, vol. 83, no. 2, pp. 253–264, 1961.

[10] S. Strommer, A. Steinboeck, C. Begle, M. Niederer, and A. Kugi, "Modeling and control of gas supply for burners in gas-fired industrial furnaces," in *Proceedings of the IEEE Conference on Control Applications (CCA)*, Antibes, France, 2014, pp. 210–215.

[11] J. C. Strikwerda, *Finite Difference Schemes and Partial Differential Equations*, 2nd ed. Philadelphia: SIAM, 2004.

[12] A. Steinboeck, D. Wild, T. Kiefer, and A. Kugi, "A fast simulation method for 1D heat conduction," *Mathematics and Computers in Simulation*, vol. 82, no. 3, pp. 392–403, 2011.

[13] W. Yu, W. Liu, Y. Lai, L. Chen, and X. Yi, "Nonlinear analysis of coupled temperature-seepage problem of warm oil pipe in permafrost regions of Northeast China," *Applied Thermal Engineering*, vol. 70, no. 1, pp. 988–995, 2014.

[14] H. Murrenhoff, *Fundamentals of Fluid Power: 2: Pneumatics*. Aachen: Shaker Verlag, 2014.

[15] P. Beater, *Pneumatic Drives: System Design, Modelling and Control*. Berlin, Heidelberg: Springer, 2007.

[16] D. McCloy and H. R. Martin, *Control of Fluid Power: Analysis and Design*, 2nd ed. Hoboken: John Wiley & Sons, 1980.

[17] W. Wagner, *Strömung und Druckverlust*, 6th ed. Würzburg: Vogel, 2008.

[18] B. S. Petukhov, "Heat transfer and friction in turbulent pipe flow with variable physical properties," *Advances in Heat Transfer*, vol. 6, pp. 503–564, 1970.

[19] H. D. Baehr and K. Stephan, *Heat and Mass Transfer*, 2nd ed. Berlin, Heidelberg: Springer, 2006.

[20] T. L. Bergman, A. S. Lavine, F. P. Incropera, and D. P. DeWitt, *Introduction to Heat Transfer*, 6th ed. Hoboken: John Wiley & Sons, 2007.

[21] C. A. J. Fletcher, *Computational Galerkin Methods*. New York, Philadelphia: Springer, 1984.

[22] C. Fröhlich, "Media supply of gas burners of a direct-fired furnace," Master's thesis, Automation and Control Institute (ACIN), TU Wien, Vienna, 2015.

[23] L. Tsikonis, J. Van herle, and D. Favrat, "The error in gas temperature measurements with thermocouples: Application on an SOFC system heat exchanger," *Fuel Cells*, vol. 12, no. 1, pp. 32–40, 2012.

[24] L. Michalski, K. Eckersdorf, J. Kucharski, and J. McGhee, *Temperature Measurement*. Chichester: John Wiley & Sons, 2001.

[25] R. Schafer, "What is a Savitzky-Golay filter?" *IEEE Signal Processing Magazine*, vol. 28, no. 4, pp. 111–117, 2011.

Post-print version of the article: C. Froehlich, S. Strommer, A. Steinboeck, M. Niederer, and A. Kugi, "Modeling of the media supply of gas burners of an industrial furnace", *IEEE Transactions on Industry Applications*, vol. 52, no. 3, pp. 2664–2672, May 2016. DOI: 10.1109/TIA.2016.2521738
The content of this post-print version is identical to the published paper but without the publisher's final layout or copy editing.